HHS Public Access

Author manuscript

Dev Cell. Author manuscript; available in PMC 2016 January 12.

Published in final edited form as:

Dev Cell. 2015 January 12; 32(1): 97–108. doi:10.1016/j.devcel.2014.11.018.

Reverse genetic screening reveals poor correlation between Morpholino-induced and mutant phenotypes in zebrafish

F. O. Kok[#1], **M. Shin**[#1], **C-W. Ni**[#1,8], **A. Gupta**[1], **A. S. Grosse**[1], **A. van Impel**[2], **B. C. Kirchmaier**[2,9], **J. Peterson-Maduro**[2], **G. Kourkoulis**[1], **I. Male**[1], **D.F. DeSantis**[1], **S. Sheppard-Tindell**[1], **L. Ebarasi**[3,4], **C. Betsholtz**[3,4], **S. Schulte-Merker**[2,5], **S. A. Wolfe**[1,6], and **N. D. Lawson**[1,*]

[1] Program in Gene Function and Expression, University of Massachusetts Medical School, Worcester, MA 01605, USA [2] Hubrecht Institute – KNAW & UMC Utrecht, 3584CT Utrecht, Netherlands [3] Uppsala University, Department of Immunology, Genetics, and Pathology, Rudbeck Laboratory, 751 85 Uppsala, Sweden [4] Karolinska Institute, Department of Medicinal Biochemistry and Biophysics, 171 77, Stockholm, Sweden [5] Institute for Cardiovascular Organogenesis and Regeneration, Cells-in-motion Cluster of Excellence, University of Münster, 48149 Germany [6] Department of Biochemistry and Molecular Pharmacology, University of Massachusetts Medical School, Worcester, MA 01605, USA.

[#] These authors contributed equally to this work.

SUMMARY

The widespread availability of programmable site-specific nucleases now enables targeted gene disruption in the zebrafish. In this study, we applied site-specific nucleases to generate zebrafish lines bearing individual mutations in more than twenty genes. We found that mutations in only a small proportion of genes caused defects in embryogenesis. Moreover, mutants for ten different genes failed to recapitulate published Morpholino-induced phenotypes (morphants). The absence of phenotypes in mutant embryos was not likely due to maternal effects or failure to eliminate gene function. Consistently, a comparison of published morphant defects with the Sanger Zebrafish Mutation Project revealed that approximately eighty percent of morphant phenotypes were not observed in mutant embryos, similar to our mutant collection. Based on these results, we

[*] - author for correspondence, nathan.lawson@umassmed.edu.

[8] current address: Department of Biomedical Engineering, Khalifa University of Science, Technology and Research (KUSTAR), PO BOX 127788, Abu Dhabi, UAE

[9] current address: Institute of Cell Biology and Neuroscience and Buchmann Institute for Molecular Life Sciences (BMLS), University of Frankfurt, Germany

Author Contribution. F. O. K., M. S., C-W. N., A. G. A. v. I., B. C. K., and J. P.-M. generated mutant lines and performed phenotypic analysis. A. S. G. and L. E. contributed to molecular and phenotypic characterization of the *pdgfrb* line. L. E. and C. B. provided the Pdgfrb antibody. G. K., I. M., and D. G. D. provided essential technical support, including identification of carrier fish and genotyping of embryos. S. S. T. provided support in the identification of candidate endothelial genes. N. D. L. generated the *ets1* mutant, performed molecular analyses on mutants and wrote the paper. S. S.-M. and S. A. W., along with all authors contributed to the preparation and editing of the manuscript.

suggest that mutant phenotypes become the standard metric to define gene function in zebrafish, after which Morpholinos that recapitulate respective phenotypes could be reliably applied for ancillary analyses.

INTRODUCTION

The zebrafish has become a central model system to investigate vertebrate development. Early foundational studies utilized zebrafish in large-scale forward genetic screens to identify mutants affecting different aspects of embryonic development (Driever et al., 1996; Haffter et al., 1996). These studies took advantage of the many benefits of zebrafish husbandry and embryogenesis. In particular, rapid external development of the transparent zebrafish embryo allowed detection of a range of mutant phenotypes during development. The hardy nature of zebrafish adults and their ability to produce large clutch sizes facilitated subsequent mapping of causative mutant genes (Lawson and Wolfe, 2011). These genetic screens based simply on observing embryonic morphology resulted in the discovery of genes required for distinct steps in embryogenesis, including gastrulation (Hammerschmidt et al., 1996), cardiovascular morphogenesis (Stainier et al., 1996), and hematopoiesis (Ransom et al., 1996). Subsequent forward genetic screens have been applied to dissect an array of different biological processes, ranging from immunity to digestion (Lawson and Wolfe, 2011). This work demonstrates the broad and powerful impact that the zebrafish has had as a genetic model system across multiple fields of study.

Despite the utility of forward genetics, screening to saturation in the zebrafish is challenging (Lawson and Wolfe, 2011). At the same time, the deluge of sequence data over the past decade has revealed a wealth of genes for which no mutations currently exist in zebrafish. Thus, there is a need for reverse genetic approaches to assess gene function. While not a true genetic approach, the introduction of antisense Morpholino oligomers (MOs) was initially greeted with excitement in the zebrafish community as a tool to interrogate gene function. MOs differ from standard nucleic acid oligonucleotides in that they possess a 6-ring heterocycle backbone and non-ionic phosphorodiamidate linkages (Summerton and Weller, 1997). These modifications make MOs highly stable *in vivo*, allow them to have a high affinity for RNA, and supposedly reduce their off-target binding to macromolecules (Summerton, 2007). MOs can be designed to block translation or splicing and their injection into 1-cell stage zebrafish embryos can recapitulate known mutant phenotypes (Draper et al., 2001; Nasevicius and Ekker, 2000). MOs can also block microRNA maturation and their binding to target 3’ untranslated regions (UTRs; Choi et al., 2007; Kloosterman et al., 2007). Thus, MOs provide in principle an accessible and straightforward method for gene knockdown in the zebrafish embryo.

Given their ease of use in zebrafish, MOs have enabled widespread analysis of gene function. However, MOs can induce p53-dependent apoptosis (Ekker and Larson, 2001; Pickart et al., 2006; Robu et al., 2007) and off-target cell type-specific changes in gene expression that confound phenotypic analysis (for example, see Amoyel et al., 2005; Gerety and Wilkinson, 2011). While it is possible to alleviate off-target phenotypes by simultaneously reducing p53 levels (Robu et al., 2007), the mechanism of p53 activation is

unknown. Despite this issue, anecdotal claims suggests that MOs do not share the same problems with off-target effects associated with other antisense technology, such as phosphorothioate-modified oligonucleotides (Summerton, 2007). However, there has been little empirical research in this area.

Fortunately, definitive reverse genetic approaches in zebrafish have recently become available. In particular, programmable site-specific nucleases now enable targeted gene disruption in the zebrafish. Initial work utilized zinc finger nucleases (ZFNs; Doyon et al., 2008; Meng et al., 2008) and Transcription activator-like effector nucleases (TALENs), which provide improved specificity over ZFNs, have also been developed (Cade et al., 2012). In both cases, mRNAs encoding ZFN or TALEN heterodimers are injected into 1-cell stage embryos, where they bind to their target and induce a double strand break. Imprecise repair of this break by non-homologous end joining introduces small insertions or deletions that can lead to a frameshift when targeting coding sequence; in a proportion of the embryos such lesions will occur within the germline. More recently, the programmable bacterial nuclease Cas9 has been successfully applied to introduce heritable lesions in the zebrafish genome at high frequency (Hwang et al., 2013). Together, these tools provide a robust means to generate zebrafish bearing targeted mutations in genes of interest.

A number of groups, including our own, have put significant effort toward the development and application of site-specific nucleases in zebrafish (Bedell et al., 2012; Cade et al., 2012; Chen et al., 2013; Dahlem et al., 2012; Gupta et al., 2012; Gupta et al., 2013; Hwang et al., 2013; Sander et al., 2011; Zhu et al., 2011). However, the systematic analysis of phenotypes in derived lines has lagged. In this study, we generated and characterized mutant lines for more than twenty genes. We find that the majority of these genes are dispensable for embryonic development. We also did not observe previously published MO-induced (morphant) phenotypes in ten mutant lines. A broader comparison of all published morphant phenotypes with the Sanger Zebrafish Mutation Project revealed similar discrepancies. Taken together, these observations suggest that MO off-target effects are much more prevalent than previously stated. Our results highlight the need to reevaluate the use of antisense-based technology for characterization of gene function in the zebrafish and emphasize the importance of applying targeted gene disruption for this purpose.

RESULTS

Generation of mutants in candidate genes of interest

Our general goal was to identify novel functions for genes involved in embryonic vascular development. For this purpose we applied programmable site-specific nucleases to introduce targeted deletions in candidate genes of interest identified from a number of sources (Table S1). For the most part, candidate genes were expressed in endothelial cells based on published studies, available *in situ* hybridization data at the Zebrafish Information Network (ZFIN), or identified through our own unpublished work (Table S1 and data not shown). Fourteen genes had been targeted by MOs in published work and shown to cause a developmental phenotype, including 10 that displayed a vascular or lymphatic defect (*amot*, *ccbe1*, *elmo1*, *ets1*, *flt4*, *fmnl3*, *gata2a*, *mmp2*, *nrp1a*, *pdgfrb*; Table S1). We have previously reported vascular defects in the *gata2a* mutant (Zhu et al., 2011) and it is

included here as the first mutant generated in our knockout pipeline. We also included *ccbe1* and *flt4* as "positive control" target genes for which vascular defects have already been reported in mutants from forward genetic screens (Hogan et al., 2009a; Hogan et al., 2009b).

We applied ZFNs, TALENs and, in one case, Cas9, to target genomic sequence that harbored a restriction site that could be used for genotyping and encoded amino acids in the amino-terminal half of a protein (Table S2, see below, and data not shown). We did not target near the annotated start codon to avoid alternative translational start sites, except when targeting a signal peptide (e.g. *ccbe1*, *mmp2*). We identified founder fish bearing small insertions or deletions in their germline that introduced a frameshift into the coding sequence or eliminated a splice site (Table S2). All of the lesions are expected to truncate the protein and cause non-sense mediated decay (NMD) of the mRNA transcript (see below; Table S2). For the *linc:birc6* locus, we generated a large segmental deletion. In total, we generated mutant lines bearing thirty-two distinct lesions in twenty-four genes (Table S2).

Lack of embryonic defects and discrepancy with morphant vascular phenotypes

We performed all phenotypic analysis on embryos derived from multiple in-crosses of identified heterozygous carriers of a respective mutation. In most cases, we generated families of heterozygous carriers by crossing founders with adults bearing endothelial or lymphatic endothelial transgenes to visualize vascular or lymphatic morphology, respectively (see below). We screened embryos for overt defects between 24 hours post fertilization (hpf) and 5 dpf. In parallel, we observed vascular morphology in transgenic embryos, and screened for abnormal circulatory patterns, loss of circulation, and evidence of hemorrhage. Following 5 dpf, we genotyped embryos to confirm the presence of homozygous wild type, mutant and heterozygous progeny at the expected ratios. In all cases where embryos failed to exhibit phenotypes we were able to detect genotypically mutant embryos at the expected frequency (data not shown; see examples for *ets1a*, *fam38a*, and *fmnl3* below).

In the course of phenotypic analysis, we observed defects caused by mutations in only three of the twenty-four genes. These included *gata2a*, *ccbe1* and *flt4* mutants, the latter two of which exhibited loss of the thoracic duct, a primitive lymphatic structure (Figure 1A, B) as expected from previous studies (Hogan et al., 2009a; Hogan et al., 2009b). *flt4* mutant embryos also failed to form the primordial hindbrain channel and parachordal lymphangioblasts (Figure 1B). All other mutants displayed normal overall and vascular morphology, as well as circulatory function throughout the first 5 days of development (Figure S1; Table S3, data not shown). For example, within the embryonic trunk at 30 hours post fertilization (hpf), intersegmental vessels (ISV) have completed their sprouting from the dorsal aorta (DA) and begin to form the dorsal longitudinal anastomotic vessel (DLAV) in wild type siblings (Figure 2A). The formation of these vessels has been used to screen for genes required for angiogenesis (for examples, see Covassin et al., 2009; Isogai et al., 2003; Lawson and Weinstein, 2002). We did not observe defects in vascular morphogenesis or circulatory function in any of the mutant embryos, including those bearing mutations in guanine nucleotide exchange factors (GEFs), such as *arhgef9b*, *kalrnb*, *fgd5a*, or *prex2* (Figure 2B, C, D; Table S3; data not shown), which are candidates for genes important for

endothelial migration. Most strikingly, we failed to observe defects in embryos bearing mutations in genes previously shown to be required for ISV formation using MOs (Table 1; Table S3). For example, individual MO knockdowns of *fmnl3* and *pdgfrb* cause a block in ISV sprouting (Hetheridge et al., 2012; Wiens et al., 2010). However, embryos mutant for *fmnl3*^{um150} or *pdgfrb*^{um148} display ISV growth that is indistinguishable from wild type siblings (Figure 2A, E, F). Likewise, *flt4*^{um203} mutants do not exhibit ISV stalling as we previously described in morphants (Covassin et al., 2006), despite the presence of fully penetrant lymphatic defects (Figure 1B). We noted similar defects in an extracellular domain truncation allele as well (Table S2, data not shown) and *flt4*^{um203} mutants display significantly reduced transcript levels consistent with NMD (Figure 1B) similar to *fmnl3*^{um150} (Figure 2G). RT-PCR analysis of genotypically verified heterozygous and *fmnl3*^{um150} mutant sibling embryos ruled out exon skipping and confirmed that residual mRNA transcripts bore the mutant lesion (Figure 2H, I). Likewise, *pdgfrb* transcript is reduced in *pdgfrb*^{um148} mutant embryos and Western blot analysis confirmed the absence of protein (Figure 2J, K).

Embryos bearing mutations in *amot*, *elmo1*, and *ets1* also displayed normal vascular patterning and circulatory function despite previous reports of defects in respective morphant embryos (Table S3; data not shown; Aase et al., 2007; Epting et al., 2010; Pham et al., 2007). In the case of the *ets1*^{um206} mutation, we detected transcripts missing exon 3, which contains the *um206* deletion, in heterozygous and mutant embryos (Figure 2L, M), while all remaining sequenced full-length transcripts bore the *um206* deletion (data not shown). In *ets1*, exon 3 encodes the pointed domain, which is essential for transcriptional activation by upstream kinases, such as ERK1/2 (Seidel and Graves, 2002). Thus, it is possible that *ets1*^{um206} is a hypomorphic allele. We also find that embryos bearing a truncation mutation in *neuropilin1a* (*nrp1a*; Figure 3A), a Vegf co-receptor also implicated in ISV patterning by previous studies using MO-mediated knockdown (Lee et al., 2002; Martyn and Schulte-Merker, 2004), display normal vascular patterning and circulation in the trunk blood vessels (Figure 3B, C). We did not investigate whether *pik3cg* or *smox* mutant embryos exhibited previously described morphant defects in blood cell development (Tijssen et al., 2011; Yoo et al., 2010), although both appeared normal until 5 dpf and *smox* mutant zebrafish were viable to adulthood (data not shown). Thus, for seven of the candidate genes previously implicated in ISV sprouting using MO knockdown (*amot*, *elmo1*, *ets1*, *flt4*, *fmnl3*, *nrp1a*, and *pdgfrb*), we failed to detect these defects in corresponding mutant embryos.

The discrepancies between morphant and mutant phenotypes may suggest that ISV sprouting is particularly sensitive to MO off-target effects. Therefore, we observed embryos bearing mutations in genes implicated in other aspects of development. Previous studies using MO-targeting have reported that *matrix metalloproteinase 2* (*mmp2*) is required for development of the primitive lymphatic system in zebrafish (Detry et al., 2012). We generated an allele (*mmp2*^{hu10535}) that produces a frameshift in the signal peptide and truncates the Mmp2 coding sequence (Figure 3D); a similar truncation in the signal peptide of *ccbe1* recapitulates lymphatic defects associated with previously described *ccbe1* alleles (Figure 1; Hogan et al., 2009a). By 5 days post fertilization (dpf), zebrafish larvae normally

display formation of the thoracic duct and intersegmental lymphatic vessels (ISLVs), labeled in this case by a *flt4:mCitrine* transgene, lying adjacent to intersegmental arteries expressing *flt1:tdTomato* (Figure 3E). In embryos mutant for *mmp2*^{hu10535} we similarly observed normal TD and ISLV development at this stage (Figure 3F). These results are in conflict with previous observations in morphant embryos (Detry et al., 2012) and suggest that *mmp2* may be dispensable for early lymphatic development in zebrafish.

Two of the mutant lines we generated were expected to display non-vascular phenotypes based on published morphant data. *fam38a* encodes the zebrafish homolog of Piezo1, a multi-pass transmembrane protein that functions as a mechanosensory channel (Coste et al., 2012; Kim et al., 2012b). In zebrafish, knockdown of *fam38a* using a start codon MO causes early severe morphological defects, leading to speculation that maternal contribution is important for early development (Eisenhoffer et al., 2012). Inducible knockdown at later stages using a caged MO leads to epidermal masses in the developing fin fold due to defects in cell extrusion (Eisenhoffer et al., 2012). However, separate studies using both translational and splice-targeting MOs reported specific defects in red blood cell volume, similar to human patients bearing gain of function mutations in *PIEZO1* (Faucherre et al., 2014), but no overt defects. The *fam38a*^{um136} mutant is a frameshift leading to truncation of the Fam38a coding sequence at amino acid 361 (Figure 4A; Table S2). Consistent with NMD, we observe that *fam38a* transcript is reduced in *fam38a*^{um136} mutant embryos compared to wild type siblings (Figure 4B, C). RT-PCR analysis of residual *fam38a* transcript from mutant embryos did not reveal exon skipping or presence of wild type transcripts (Figure 4D-F). Interestingly, we noted a low frequency of deletions larger than the *um136* lesion suggesting that this microdeletion affects splicing, although all deletions in the transcript resulted in a frameshift (Figure 4G). Despite the presence of this mutation, fin morphology was indistinguishable between wild type and *fam38a*^{um136} mutant sibling embryos at 72 hpf (Figure 5H, I). Together with the discrepancies between published reports utilizing a translation-blocking MO, these results suggest that the overt gastrulation and fin defects from previous studies (Eisenhoffer et al., 2012) may have been due to off-target effects.

The mutants described above bear frameshifts and in selected cases we observe evidence of NMD or loss of protein. However, we have also noted exon skipping and possible effects on splicing. A more desirable strategy to generate a null allele would be to introduce a large deletion in a locus of interest. This approach would be particularly useful for deleting non-coding RNAs for which functional domains are difficult to identify. We have previously applied two pairs of TALENs targeting adjacent *cis* sequences to delete the locus encoding the long non-coding RNA *linc:birc6*, also referred to as *megamind* (Gupta et al., 2013; Ulitsky et al., 2011). MO-mediated knockdown of *megamind* in zebrafish causes hydrocephaly, as indicated by inflation of hindbrain ventricles (Ulitsky et al., 2011). We established a zebrafish line (*megamind*^{um209}) bearing a segmental deletion that eliminated transcripts arising from the *megamind* locus, but did not affect the *cyrano* lncRNA or expression of *eef1a1l1* mRNA (Figure 5A, B). Despite the absence of *megamind* RNA in mutant embryos, they were morphologically indistinguishable from wild type (Figure 5C, D). *megamind*^{um209} mutants were viable into adulthood and embryos derived from in-

crosses of *megamind*^{um209} homozygous adults were normal (Figure 5D). Similar results were observed for a second independent deletion of the *megamind* locus (Table S2, data not shown). The deletion in *megamind*^{um209} mutant embryos also removes the sequences targeted by published MOs (Figure 4A; (Ulitsky et al., 2011). Strikingly, injection of a previously described MO targeting *megamind* induces the appearance of inflated hindbrain ventricles in both wild type siblings and *megamind*^{um209} mutant embryos, despite the absence of the MO target site in the latter (Figure 5E, F). In this case, the MO target sequence bears only modest homology to other *megamind* paralogs within the genome (68 and 76 percent). We would point out that similar phenotypes were observed with splice site MOs that would not be expected to target these other long non-coding RNAs (Ulitsky et al., 2011). The MO would also not be expected to reduce expression of the related *tuna* long non-coding RNA that has recently been implicated in brain development in zebrafish (Lin et al., 2014). Thus, these observations suggest that the previously reported *megamind* phenotype is likely due to MO off-target effects.

Evidence of a high false-positive rate for morphant phenotypes

Our results suggest that many morphant phenotypes are not recapitulated in mutant embryos. To assess how universal this finding might be we performed an integrative analysis of curated datasets available from ZFIN and the Sanger Zebrafish Mutation Project (ZMP), which has reported phenotypic analysis of mutant embryos for more than 700 genes (Kettleborough et al., 2013). We identified 98 ZMP mutants for which morphant phenotypes have been published. We restricted analysis to overt morphant phenotypes that affected the whole embryo and would have been easily seen in the ZMP phenotyping pipeline. We further performed literature-based validation of ZFIN data and eliminated any ZMP mutants unlikely to affect protein function (Table S4) to yield 24 genes for comparison (Table S5). Mutations in only 5 of these genes resulted in observable phenotypes that were largely consistent with MO knockdown experiments, while the rest did not (Figure 6, Table 1; Table S5). We did not note any obvious pattern in effective dosage, rescue penetrance, p53 rescue, or other variable that predicted whether a MO would yield a discordant phenotype (Table S3, S5).

The discrepancies between morphants and mutants may be due to the use of a MO targeting the start codon, which blocks translation of maternal mRNAs, while mutant embryos derived from heterozygotes lack only zygotic gene function. Therefore, we took into account two additional datasets: 1. nature of MO target sequence (translation, which would block maternal transcript translation, versus splice-blocking, which would affect only zygotic transcripts) used in each published study and 2. available RNA-Seq data (Harvey et al., 2013) to assess candidate mRNA levels at the 2-cell stage. We also considered studies in which maternal effects have been ruled out in published studies (e.g. *ptenb*; Faucherre et al., 2008), as well as transcript analysis and crosses of homozygous mutants in our own lines (see above; Table S3). After applying these restrictions, we identified 14 ZMP mutants and 12 in our collection where maternal contribution was unlikely (Table S3, S5; *flt4* is counted twice as it recapitulates lymphatic but not ISV defects). In these cases, 12 out of 14 Sanger mutants and 9 out of 12 of our mutants fail to exhibit published morphant phenotypes (Tables S3, S5; Figure 6). Thus, even when considering the maternal contribution, more than

70 percent of morphant phenotypes were not observed in respective mutants from two separate collections (Figure 6).

DISCUSSION

The development of programmable site-specific nucleases for genome modification now enables reverse genetic approaches to be applied in model and non-model organisms. As an initial step to broadly apply these tools in zebrafish, we have used ZFNs, TALENs and the CRISPR system to generate a collection of lines bearing mutations in candidate genes of interest. Despite the expression of most of our candidate genes in endothelial cells at early embryonic stages of development and their homology to known functional molecules, we failed to observe any notable vascular defects in mutant embryos for most of the genes analyzed. In this regard, our findings are consistent with low rates of overt phenotypes in a recent characterization of nearly 1000 zebrafish mutant lines (Kettleborough et al., 2013) and suggest a high degree of redundancy is built into the zebrafish genome.

A more troubling finding from our work is the discrepancy between morphant and mutant phenotypes. Our integrative analysis of ZMP and ZFIN datasets shows a high rate of discrepancy even when taking into account maternal contribution. A caveat here is that we restricted analysis to overt phenotypes that are also the most likely phenotypes caused by MO off-target effects. Also, some ZMP point mutants may not be null alleles. Thus, the true false-positive rate may not be as high when considering more specific defects in null mutants. However, in our mutants, which mostly bore deletions resulting in frameshifts, we focused on subtle vascular defects in a sensitive transgenic background. We also observed evidence of NMD or loss of protein in selected mutants supporting the fact that many are likely null alleles, yet we still observed a high false-positive morphant phenotype rate. Consistent with these observations, recent studies have reported inconsistencies between morphants and mutants for individual genes, including phenotypes affecting lymphatic development (*nr2f2*, Aranguren et al., 2011; Swift et al., 2014; van Impel et al., 2014), neuronal function (*mfn2* and *prp2*, Chapman et al., 2013; Fleisch et al., 2013; Nourizadeh-Lillabadi et al., 2010; Vettori et al., 2011), hindbrain patterning (*gbx2*, Kikuta et al., 2003; Su et al., 2014), and lateral line development (*tcf7*, Aman et al., 2011). Taken together with our broader findings here, these studies raise a major concern about relying solely on the application of MOs for primary characterization of gene function in the zebrafish.

Our results suggest that many morphant phenotypes may be due to off-target effects. The most striking is the *megamind* mutant, where we recapitulated the morphant phenotype in embryos lacking the MO target site. This is especially worrisome as *megamind* morphants could be rescued by co-injecting *megamind* RNA (Ulitsky et al., 2011). Likewise, five out of twelve of the morphant phenotypes that we failed to observe in mutants were rescued in previous studies (Table S3). Similar observations have recently been made for zebrafish *pak4*, which is genetically dispensable for development, despite a morphant phenotype that can be rescued by mRNA injection (Law and Sargent, 2014). Given the high copy number of injected MO (10 ng of a MO is equal to approximately 6.3×10^{11} molecules), as well as the rescue RNA, which is typically co-injected, it is possible that non-specific interference of the co-injected RNA with the MO may lead to reduced knockdown efficiency and

apparent rescue. Most studies also fail to confirm that endogenous protein or transcript is similarly affected by MO injection in both the absence and presence of rescue mRNA. Thus, current methods of rescue for morphant phenotypes are not a reliable guideline for verification of MO specificity.

MO off-target effects have been attributed to p53 induction that leads to apoptosis (Robu et al., 2007) and can cause seemingly specific gene expression changes in certain cell types (Amoyel et al., 2005; Gerety and Wilkinson, 2011). However, little is known concerning the mechanism by which MOs induce p53 activation. While characteristics of the MO backbone are thought to reduce interactions with macromolecules, there are only anecdotal claims to this effect (Summerton, 2007) and no studies have investigated off-target effects independent of RNA binding. Furthermore, MOs bearing up to 4 base mismatches can effectively inhibit target mRNA, suggesting a wide spectrum of off-target RNA binding. Thus, more global effects on translation, splicing, and, possibly, small RNA processing are possible. This, in turn, could trigger the induction of p53. In this case, p53 knockdown would only ameliorate some of the observed off-target effects. Notably, a recent study demonstrates that a morphant phenotype not rescued by p53 knockdown, and therefore thought to be specifically caused by knockdown of the target gene, was also not seen in the corresponding null maternal/zygotic mutant (Law and Sargent, 2014). Thus, similar to mRNA injection, p53 knockdown may not be a reliable indicator for the specificity of a morphant phenotype. If MOs are to be applied as a tool in parallel with targeted gene knockout to discern gene function, further studies are clearly needed to clarify the mechanism of off-target responses.

The ability to knock down candidate genes of interest using MOs clearly had an impactful role in the application of the zebrafish as a model system. Indeed, nearly 300 morphant phenotypes curated in ZFIN are consistent with those observed in mutant embryos (unpublished observation), as are several in the current study. However, there have long been anecdotal claims within the zebrafish community of problematic p53-independent off-target effects and variability due to different preparations of the same MO. Based on these reports, Drs. Judith Eisen and James Smith published a list of guidelines for the reliable application of MOs in frog and zebrafish in 2008 (Eisen and Smith, 2008). Among their recommendations was that, whenever possible, investigators confirm a morphant phenotype by comparison to a mutant, if available. Our findings here suggest that this is the most essential guideline to follow. At the same time, it is also important to validate the characteristics of newly generated mutant lines in parallel to confirm their effect on candidate gene function. Indeed, we noted cases of exon skipping and splicing defects in some mutants. Moving forward, we recommend targeting exons encoding domains that are necessary for protein function or generating segmental deletions. Given the ease of use of current site-specific nuclease technologies, most notably the CRISPR systems, we would advocate for widespread application of these approaches to generate mutants. While this approach requires a significant research investment (typically between 6 to 12 months from initial injections to phenotypic characterization of mutant phenotypes), our observations clearly demonstrate the need for a genetic approach as the definitive determination of gene function. Moreover, we would suggest broader community-wide and editorial guidelines that require an observed MO-induced phenotype to be validated in embryos bearing

mutations in the same gene, after which a MO could then be reliably applied for subsequent functional studies.

EXPERIMENTAL PROCEDURES

Zebrafish Handling and Maintenance

Zebrafish were maintained in accordance with approved institutional protocols at the University of Massachusetts Medical School and the Hubrecht Institute. The *Tg(fli1a:egfp)*^{y1}, *Tg(kdrl:egfp)*^{s843}, *Tg(gata1a:dsRed)*^{sd2}, *Tg(flt4:mCitrine)*^{hu7135}, and *Tg(flt1:tdTomato)*^{hu5333} transgenic lines have been described elsewhere (Beis et al., 2005; Bussmann et al., 2010; Lawson and Weinstein, 2002; Traver et al., 2003; van Impel et al., 2014).

Construction of site-specific nucleases

Zinc finger nucleases (ZFNs) or TAL effector nucleases (TALENs) were constructed as described elsewhere (Kok et al., 2014). Appropriate zinc finger cassettes and target sites were identified in candidate genes using previously described databases of targets identified in the zebrafish genome (Gupta et al., 2012; Zhu et al., 2011). TALEN sequences were identified in candidate genes using TAL effector Nucleotide Targeter 2.0 (https://tale-nt.cac.cornell.edu/). The list of target sites within candidate genes can be found in Table S2. All nuclease sequences are available upon request. Generation of mutant lines was performed as described elsewhere (Kok et al., 2014; Meng et al., 2008; Gupta et al., 2013). A sgRNA targeting *ets1* (Table S2) was chosen based on location in a functional domain and presence of restriction enzyme site useful for genotyping. sgRNA was synthesized and used to generate mutant founders based on published protocols (Gagnon et al., 2014).

Phenotypic analysis

Embryos derived from identified heterozygous carriers were observed every day for the first 5 days of development using a dissection microscope. Transmitted light and DIC images, as well as analysis of vascular or lymphatic morphology using confocal or 2-photon microscopy were performed as described elsewhere (Quillien et al., 2014; van Impel et al., 2014). In some cases, transgenic embryos were fixed and subjected to immunostaining with GFP antibody to boost the fluorescent signal, as we have done previously (Covassin et al., 2006). All embryos were subsequently subjected to individual genotypic analysis, which was performed using restriction digest of PCR fragments encompassing the targeted sequence as we have done previously (Meng et al., 2008).

RT-PCR and Western blot analysis.—We performed RT-PCR or Western blot analysis on wild type and mutant sibling embryos as follows: individual embryos were anesthetized according to standard protocols, their heads were removed using a scalpel, and transferred to an individual well of a 96-well plate. In parallel, the trunk region was transferred to individual Eppendorf tubes in a dry ice/ethanol bath and subsequently stored at −80°C. Embryo heads were used for genomic DNA isolation and genotype analysis as described previously (Meng et al., 2008). Several trunks of genotypically identical embryos were pooled and dissociated in Trizol, or lysed in sample buffer for protein isolation. Reverse

transcription of total RNA was performed using oligo-dT and Superscript III (Invitrogen) according to manufacturer's protocols. PCR was performed using primers listed in Supplemental Experimental Procedures. PCR fragments from genomic DNA were directly sequenced, while those from cDNA were cloned into pGEM-T (Promega) prior to sequencing. Western blot analysis was performed according to standard protocols. An antibody against zebrafish Pdgfrb was raised in rabbits (Innovagen, Lund, Sweden) using a synthetic peptide (KYADIQPSPYESPYQQDIYQ).

Riboprobes—Fragments for synthesizing riboprobes were amplified from wild type cDNA and cloned into pGEM-T by TA cloning (Promega). Oligonucleotide primers are listed in Supplemental Experimental Procedures. To generate digoxigenin labeled antisense riboprobes, DNA templates were first generated from plasmids using M13 forward and reverse primers. Templates were purified by ethanol precipitation and used for *in vitro* transcription using the appropriate bacteriophage RNA polymerase. The riboprobe against *pdgfrb* was prepared by linearizing the template plasmid with Apa I prior to synthesis with RNA polymerase.

Integration of Sanger and ZFIN datasets—We downloaded the list of phenotyped mutants generated through the Sanger Zebrafish Mutation resource from the Sanger Center website (http://www.sanger.ac.uk/sanger/Zebrafish_Zmpbrowse). We downloaded and extracted all morphant data from the Zebrafish Information Network (http://zfin.org/downloads/phenoGeneCleanData.txt). Both downloads were done in April 2014. Datasets were cross-referenced to identify genes for which MO-mediated knockdown resulted in a phenotype and a corresponding mutant had been subjected to phenotypic analysis (98 genes). We next restricted analysis to only whole embryos phenotypes, (Field = "_Affected_structure_or_Process_1_superterm_Name", term = "whole organism"), yielding 33 genes. This list was subsequently hand annotated through primary literatures searches to confirm that curated ZFIN data was accurate. From this analysis, we eliminated 4 genes that gave subtle morphant phenotypes, and 1 gene that did not recapitulate the phenotype of a previously existing mutant. We further removed 4 genes that were less likely to bear severely mutagenic alleles (Table S4). To assess maternal contribution, we integrated published RNA-Seq data (Harvey et al., 2013) and verified application of translation or splice blocking MOs from the primary literature in each case. We also took into account other published sources investigating genetic maternal requirement, including our observations in this study. Genes for which fragments per kilobase per million (FPKM) was 0, or which displayed a phenotype with a splice-blocking MO, were classified as "unlikely" to contribute maternal function. All others were classified as "possible".

Supplementary Material

Refer to Web version on PubMed Central for supplementary material.

Acknowledgements

This work was funded by grants to N. L. (R01HL079266, R01HL101374) and a multi-PI grant to N.L. and S. A. W. (R01HL093766) from the National Heart, Lung, and Blood Institute. S. S.-M. was supported by the Deutsche

Forschungsgemeinschaft (DFG), Cells-in-Motion Cluster of Excellence (EXC 1003 – CiM), University of Münster, Germany.

REFERENCES

Aase K, Ernkvist M, Ebarasi L, Jakobsson L, Majumdar A, Yi C, Birot O, Ming Y, Kvanta A, Edholm D, et al. Angiomotin regulates endothelial cell migration during embryonic angiogenesis. Genes & development. 2007; 21:2055–2068. [PubMed: 17699752]

Aman A, Nguyen M, Piotrowski T. Wnt/beta-catenin dependent cell proliferation underlies segmented lateral line morphogenesis. Dev Biol. 2011; 349:470–482. [PubMed: 20974120]

Amoyel M, Cheng YC, Jiang YJ, Wilkinson DG. Wnt1 regulates neurogenesis and mediates lateral inhibition of boundary cell specification in the zebrafish hindbrain. Development. 2005; 132:775–785. [PubMed: 15659486]

Aranguren XL, Beerens M, Vandevelde W, Dewerchin M, Carmeliet P, Luttun A. Transcription factor COUP-TFII is indispensable for venous and lymphatic development in zebrafish and Xenopus laevis. Biochem Biophys Res Commun. 2011; 410:121–126. [PubMed: 21641336]

Bedell VM, Wang Y, Campbell JM, Poshusta TL, Starker CG, Krug RG 2nd, Tan W, Penheiter SG, Ma AC, Leung AY, et al. In vivo genome editing using a high-efficiency TALEN system. Nature. 2012; 491:114–118. [PubMed: 23000899]

Beis D, Bartman T, Jin SW, Scott IC, D'Amico LA, Ober EA, Verkade H, Frantsve J, Field HA, Wehman A, et al. Genetic and cellular analyses of zebrafish atrioventricular cushion and valve development. Development. 2005; 132:4193–4204. [PubMed: 16107477]

Bussmann J, Bos FL, Urasaki A, Kawakami K, Duckers HJ, Schulte-Merker S. Arteries provide essential guidance cues for lymphatic endothelial cells in the zebrafish trunk. Development. 2010; 137:2653–2657. [PubMed: 20610484]

Cade L, Reyon D, Hwang WY, Tsai SQ, Patel S, Khayter C, Joung JK, Sander JD, Peterson RT, Yeh JR. Highly efficient generation of heritable zebrafish gene mutations using homo- and heterodimeric TALENs. Nucleic Acids Res. 2012; 40:8001–8010. [PubMed: 22684503]

Cha YI, Kim SH, Sepich D, Buchanan FG, Solnica-Krezel L, DuBois RN. Cyclooxygenase-1-derived PGE2 promotes cell motility via the G-protein-coupled EP4 receptor during vertebrate gastrulation. Genes & development. 2006; 20:77–86. [PubMed: 16391234]

Chapman AL, Bennett EJ, Ramesh TM, De Vos KJ, Grierson AJ. Axonal Transport Defects in a Mitofusin 2 Loss of Function Model of Charcot-Marie-Tooth Disease in Zebrafish. PLoS One. 2013; 8:e67276. [PubMed: 23840650]

Chen S, Oikonomou G, Chiu CN, Niles BJ, Liu J, Lee DA, Antoshechkin I, Prober DA. A large-scale in vivo analysis reveals that TALENs are significantly more mutagenic than ZFNs generated using context-dependent assembly. Nucleic Acids Res. 2013; 41:2769–2778. [PubMed: 23303782]

Choi WY, Giraldez AJ, Schier AF. Target protectors reveal dampening and balancing of Nodal agonist and antagonist by miR-430. Science. 2007; 318:271–274. [PubMed: 17761850]

Coste B, Xiao B, Santos JS, Syeda R, Grandl J, Spencer KS, Kim SE, Schmidt M, Mathur J, Dubin AE, et al. Piezo proteins are pore-forming subunits of mechanically activated channels. Nature. 2012; 483:176–181. [PubMed: 22343900]

Covassin LD, Siekmann AF, Kacergis MC, Laver E, Moore JC, Villefranc JA, Weinstein BM, Lawson ND. A genetic screen for vascular mutants in zebrafish reveals dynamic roles for Vegf/Plcg1 signaling during artery development. Dev Biol. 2009; 329:212–226. [PubMed: 19269286]

Covassin LD, Villefranc JA, Kacergis MC, Weinstein BM, Lawson ND. Distinct genetic interactions between multiple Vegf receptors are required for development of different blood vessel types in zebrafish. Proc Natl Acad Sci U S A. 2006; 103:6554–6559. [PubMed: 16617120]

Croushore JA, Blasiole B, Riddle RC, Thisse C, Thisse B, Canfield VA, Robertson GP, Cheng KC, Levenson R. Ptena and ptenb genes play distinct roles in zebrafish embryogenesis. Dev Dyn. 2005; 234:911–921. [PubMed: 16193492]

Dahlem TJ, Hoshijima K, Jurynec MJ, Gunther D, Starker CG, Locke AS, Weis AM, Voytas DF, Grunwald DJ. Simple methods for generating and detecting locus-specific mutations induced with TALENs in the zebrafish genome. PLoS Genet. 2012; 8:e1002861. [PubMed: 22916025]

Detry B, Erpicum C, Paupert J, Blacher S, Maillard C, Bruyere F, Pendeville H, Remacle T, Lambert V, Balsat C, et al. Matrix metalloproteinase-2 governs lymphatic vessel formation as an interstitial collagenase. Blood. 2012; 119:5048–5056. [PubMed: 22490679]

Doyon Y, McCammon JM, Miller JC, Faraji F, Ngo C, Katibah GE, Amora R, Hocking TD, Zhang L, Rebar EJ, et al. Heritable targeted gene disruption in zebrafish using designed zinc-finger nucleases. Nat Biotechno. 2008; l26:702–708.

Draper BW, Morcos PA, Kimmel CB. Inhibition of zebrafish fgf8 pre-mRNA splicing with morpholino oligos: a quantifiable method for gene knockdown. Genesis. 2001; 30:154–156. [PubMed: 11477696]

Driever W, Solnica-Krezel L, Schier AF, Neuhauss SC, Malicki J, Stemple DL, Stainier DY, Zwartkruis F, Abdelilah S, Rangini Z, et al. A genetic screen for mutations affecting embryogenesis in zebrafish. Development. 1996; 123:37–46. [PubMed: 9007227]

Eisen JS, Smith JC. Controlling morpholino experiments: don't stop making antisense. Development. 2008; 135:1735–1743. [PubMed: 18403413]

Eisenhoffer GT, Loftus PD, Yoshigi M, Otsuna H, Chien CB, Morcos PA, Rosenblatt J. Crowding induces live cell extrusion to maintain homeostatic cell numbers in epithelia. Nature. 2012; 484:546–549. [PubMed: 22504183]

Ekker SC, Larson JD. Morphant technology in model developmental systems. Genesis. 2001; 30:89–93. [PubMed: 11477681]

Epting D, Wendik B, Bennewitz K, Dietz CT, Driever W, Kroll J. The Rac1 regulator ELMO1 controls vascular morphogenesis in zebrafish. Circulation research. 2010; 107:45–55. [PubMed: 20466982]

Faucherre A, Kissa K, Nargeot J, Mangoni ME, Jopling C. Piezo1 plays a role in erythrocyte volume homeostasis. Haematologica. 2014; 99:70–75. [PubMed: 23872304]

Faucherre A, Taylor GS, Overvoorde J, Dixon JE, Hertog J. Zebrafish pten genes have overlapping and non-redundant functions in tumorigenesis and embryonic development. Oncogene. 2008; 27:1079–1086. [PubMed: 17704803]

Fiedler J, Jazbutyte V, Kirchmaier BC, Gupta SK, Lorenzen J, Hartmann D, Galuppo P, Kneitz S, Pena JT, Sohn-Lee C, et al. MicroRNA-24 regulates vascularity after myocardial infarction. Circulation. 2011; 124:720–730. [PubMed: 21788589]

Fleisch VC, Leighton PL, Wang H, Pillay LM, Ritzel RG, Bhinder G, Roy B, Tierney KB, Ali DW, Waskiewicz AJ, et al. Targeted mutation of the gene encoding prion protein in zebrafish reveals a conserved role in neuron excitability. Neurobiol Dis. 2013; 55:11–25. [PubMed: 23523635]

Gagnon JA, Valen E, Thyme SB, Huang P, Ahkmetova L, Pauli A, Montague TG, Zimmerman S, Richter C, Schier AF. Efficient mutagenesis by Cas9 protein-mediated oligonucleotide insertion and large-scale assessment of single-guide RNAs. PLoS One. 2014; 9:e98186. [PubMed: 24873830]

Gerety SS, Wilkinson DG. Morpholino artifacts provide pitfalls and reveal a novel role for pro-apoptotic genes in hindbrain boundary development. Dev Biol. 2011; 350:279–289. [PubMed: 21145318]

Gupta A, Christensen RG, Rayla AL, Lakshmanan A, Stormo GD, Wolfe SA. An optimized two-finger archive for ZFN-mediated gene targeting. Nature methods. 2012; 9:588–590. [PubMed: 22543349]

Gupta A, Hall VL, Kok FO, Shin M, McNulty JC, Lawson ND, Wolfe SA. Targeted chromosomal deletions and inversions in zebrafish. Genome Res. 2013; 23:1008–1017. [PubMed: 23478401]

Haffter P, Granato M, Brand M, Mullins MC, Hammerschmidt M, Kane DA, Odenthal J, van Eeden FJ, Jiang YJ, Heisenberg CP, et al. The identification of genes with unique and essential functions in the development of the zebrafish, Danio rerio. Development. 1996; 123:1–36. [PubMed: 9007226]

Hammerschmidt M, Pelegri F, Mullins MC, Kane DA, Brand M, van Eeden FJ, Furutani-Seiki M, Granato M, Haffter P, Heisenberg CP, et al. Mutations affecting morphogenesis during gastrulation and tail formation in the zebrafish, Danio rerio. Development. 1996; 123:143–151. [PubMed: 9007236]

Harvey SA, Sealy I, Kettleborough R, Fenyes F, White R, Stemple D, Smith JC. Identification of the zebrafish maternal and paternal transcriptomes. Development. 2013; 140:2703–2710. [PubMed: 23720042]

Hetheridge C, Scott AN, Swain RK, Copeland JW, Higgs HN, Bicknell R, Mellor H. The formin FMNL3 is a cytoskeletal regulator of angiogenesis. Journal of cell science. 2012; 125:1420–1428. [PubMed: 22275430]

Hillman RT, Feng BY, Ni J, Woo WM, Milenkovic L, Hayden Gephart MG, Teruel MN, Oro AE, Chen JK, Scott MP. Neuropilins are positive regulators of Hedgehog signal transduction. Genes & development. 2011; 25:2333–2346. [PubMed: 22051878]

Hogan BM, Bos FL, Bussmann J, Witte M, Chi NC, Duckers HJ, Schulte-Merker S. Ccbe1 is required for embryonic lymphangiogenesis and venous sprouting. Nature genetics. 2009a; 41:396–398. [PubMed: 19287381]

Hogan BM, Herpers R, Witte M, Helotera H, Alitalo K, Duckers HJ, Schulte-Merker S. Vegfc/Flt4 signalling is suppressed by Dll4 in developing zebrafish intersegmental arteries. Development. 2009b; 136:4001–4009. [PubMed: 19906867]

Hwang WY, Fu Y, Reyon D, Maeder ML, Tsai SQ, Sander JD, Peterson RT, Yeh JR, Joung JK. Efficient genome editing in zebrafish using a CRISPR-Cas system. Nat Biotechnol. 2013; 31:227–229. [PubMed: 23360964]

Isken A, Holzschuh J, Lampert JM, Fischer L, Oberhauser V, Palczewski K, von Lintig J. Sequestration of retinyl esters is essential for retinoid signaling in the zebrafish embryo. The Journal of biological chemistry. 2007; 282:1144–1151. [PubMed: 17098734]

Isogai S, Lawson ND, Torrealday S, Horiguchi M, Weinstein BM. Angiogenic network formation in the developing vertebrate trunk. Development. 2003; 130:5281–5290. [PubMed: 12954720]

Kettleborough RN, Busch-Nentwich EM, Harvey SA, Dooley CM, de Bruijn E, van Eeden F, Sealy I, White RJ, Herd C, Nijman IJ, et al. A systematic genome-wide analysis of zebrafish protein-coding gene function. Nature. 2013; 496:494–497. [PubMed: 23594742]

Kikuta H, Kanai M, Ito Y, Yamasu K. gbx2 Homeobox gene is required for the maintenance of the isthmic region in the zebrafish embryonic brain. Dev Dyn. 2003; 228:433–450. [PubMed: 14579382]

Kim GY, Kim HY, Kim HT, Moon JM, Kim CH, Kang S, Rhim H. HtrA1 is a novel antagonist controlling fibroblast growth factor (FGF) signaling via cleavage of FGF8. Mol Cell Biol. 2012a; 32:4482–4492. [PubMed: 22949504]

Kim SE, Coste B, Chadha A, Cook B, Patapoutian A. The role of Drosophila Piezo in mechanical nociception. Nature. 2012b; 483:209–212. [PubMed: 22343891]

Kloosterman WP, Lagendijk AK, Ketting RF, Moulton JD, Plasterk RH. Targeted inhibition of miRNA maturation with morpholinos reveals a role for miR-375 in pancreatic islet development. PLoS Biol. 2007; 5:e203. [PubMed: 17676975]

Kok FO, Gupta A, Lawson ND, Wolfe SA. Construction and application of site-specific artificial nucleases for targeted gene editing. Methods Mol Biol. 2014; 1101:267–303. [PubMed: 24233786]

Law SH, Sargent TD. The serine-threonine protein kinase PAK4 is dispensable in zebrafish: identification of a morpholino-generated pseudophenotype. PLoS One. 2014; 9:e100268. [PubMed: 24945275]

Lawson ND, Weinstein BM. In vivo imaging of embryonic vascular development using transgenic zebrafish. Dev Biol. 2002; 248:307–318. [PubMed: 12167406]

Lawson ND, Wolfe SA. Forward and reverse genetic approaches for the analysis of vertebrate development in the zebrafish. Dev Cell. 2011; 21:48–64. [PubMed: 21763608]

Lee P, Goishi K, Davidson AJ, Mannix R, Zon L, Klagsbrun M. Neuropilin-1 is required for vascular development and is a mediator of VEGF-dependent angiogenesis in zebrafish. Proc Natl Acad Sci U S A. 2002; 99:10470–10475. [PubMed: 12142468]

Lele Z, Bakkers J, Hammerschmidt M. Morpholino phenocopies of the swirl, snailhouse, somitabun, minifin, silberblick, and pipetail mutations. Genesis. 2001; 30:190–194. [PubMed: 11477706]

Lin N, Chang KY, Li Z, Gates K, Rana ZA, Dang J, Zhang D, Han T, Yang CS, Cunningham TJ, et al. An evolutionarily conserved long noncoding RNA TUNA controls pluripotency and neural lineage commitment. Mol Cell. 2014; 53:1005–1019. [PubMed: 24530304]

Majczenko K, Davidson AE, Camelo-Piragua S, Agrawal PB, Manfready RA, Li X, Joshi S, Xu J, Peng W, Beggs AH, et al. Dominant mutation of CCDC78 in a unique congenital myopathy with prominent internal nuclei and atypical cores. Am J Hum Genet. 2012; 91:365–371. [PubMed: 22818856]

Mangos S, Lam PY, Zhao A, Liu Y, Mudumana S, Vasilyev A, Liu A, Drummond IA. The ADPKD genes pkd1a/b and pkd2 regulate extracellular matrix formation. Dis Model Mech. 2010; 3:354–365. [PubMed: 20335443]

Martyn U, Schulte-Merker S. Zebrafish neuropilins are differentially expressed and interact with vascular endothelial growth factor during embryonic vascular development. Dev Dyn. 2004; 231:33–42. [PubMed: 15305285]

Meng X, Noyes MB, Zhu LJ, Lawson ND, Wolfe SA. Targeted gene inactivation in zebrafish using engineered zinc-finger nucleases. Nat Biotechnol. 2008; 26:695–701. [PubMed: 18500337]

Moser M, Yu Q, Bode C, Xiong JW, Patterson C. BMPER is a conserved regulator of hematopoietic and vascular development in zebrafish. J Mol Cell Cardiol. 2007; 43:243–253. [PubMed: 17618647]

Nasevicius A, Ekker SC. Effective targeted gene 'knockdown' in zebrafish. Nat Genet. 2000; 26:216–220. [PubMed: 11017081]

Nishibori Y, Katayama K, Parikka M, Oddsson A, Nukui M, Hultenby K, Wernerson A, He B, Ebarasi L, Raschperger E, et al. Glcci1 deficiency leads to proteinuria. J Am Soc Nephrol. 2011; 22:2037–2046. [PubMed: 21949092]

Nourizadeh-Lillabadi R, Seilo Torgersen J, Vestrheim O, Konig M, Alestrom P, Syed M. Early embryonic gene expression profiling of zebrafish prion protein (Prp2) morphants. PLoS One. 2010; 5:e13573. [PubMed: 21042590]

Parsons MJ, Campos I, Hirst EM, Stemple DL. Removal of dystroglycan causes severe muscular dystrophy in zebrafish embryos. Development. 2002a; 129:3505–3512. [PubMed: 12091319]

Parsons MJ, Pollard SM, Saude L, Feldman B, Coutinho P, Hirst EM, Stemple DL. Zebrafish mutants identify an essential role for laminins in notochord formation. Development. 2002b; 129:3137–3146. [PubMed: 12070089]

Pei W, Williams PH, Clark MD, Stemple DL, Feldman B. Environmental and genetic modifiers of squint penetrance during zebrafish embryogenesis. Dev Biol. 2007; 308:368–378. [PubMed: 17583692]

Pham VN, Lawson ND, Mugford JW, Dye L, Castranova D, Lo B, Weinstein BM. Combinatorial function of ETS transcription factors in the developing vasculature. Dev Biol. 2007; 303:772–783. [PubMed: 17125762]

Pickart MA, Klee EW, Nielsen AL, Sivasubbu S, Mendenhall EM, Bill BR, Chen E, Eckfeldt CE, Knowlton M, Robu ME, et al. Genome-wide reverse genetics framework to identify novel functions of the vertebrate secretome. PLoS One. 2006; 1:e104. [PubMed: 17218990]

Quillien A, Moore JC, Shin M, Siekmann AF, Smith T, Pan L, Moens CB, Parsons MJ, Lawson ND. Distinct Notch signaling outputs pattern the developing arterial system. Development. 2014; 141:1544–1552. [PubMed: 24598161]

Ransom DG, Haffter P, Odenthal J, Brownlie A, Vogelsang E, Kelsh RN, Brand M, van Eeden FJ, Furutani-Seiki M, Granato M, et al. Characterization of zebrafish mutants with defects in embryonic hematopoiesis. Development. 1996; 123:311–319. [PubMed: 9007251]

Robu ME, Larson JD, Nasevicius A, Beiraghi S, Brenner C, Farber SA, Ekker SC. p53 activation by knockdown technologies. PLoS Genet. 2007; 3:e78. [PubMed: 17530925]

San Antonio JD, Zoeller JJ, Habursky K, Turner K, Pimtong W, Burrows M, Choi S, Basra S, Bennett JS, DeGrado WF, et al. A key role for the integrin alpha2beta1 in experimental and developmental angiogenesis. Am J Pathol. 2009; 175:1338–1347. [PubMed: 19700757]

Sander JD, Dahlborg EJ, Goodwin MJ, Cade L, Zhang F, Cifuentes D, Curtin SJ, Blackburn JS, Thibodeau-Beganny S, Qi Y, et al. Selection-free zinc-finger-nuclease engineering by context-dependent assembly (CoDA). Nature methods. 2011; 8:67–69. [PubMed: 21151135]

Sayer JA, Otto EA, O'Toole JF, Nurnberg G, Kennedy MA, Becker C, Hennies HC, Helou J, Attanasio M, Fausett BV, et al. The centrosomal protein nephrocystin-6 is mutated in Joubert syndrome and activates transcription factor ATF4. Nature genetics. 2006; 38:674–681. [PubMed: 16682973]

Schenck A, Goto-Silva L, Collinet C, Rhinn M, Giner A, Habermann B, Brand M, Zerial M. The endosomal protein Appl1 mediates Akt substrate specificity and cell survival in vertebrate development. Cell. 2008; 133:486–497. [PubMed: 18455989]

Seeley M, Huang W, Chen Z, Wolff WO, Lin X, Xu X. Depletion of zebrafish titin reduces cardiac contractility by disrupting the assembly of Z-discs and A-bands. Circulation research. 2007; 100:238–245. [PubMed: 17170364]

Seidel JJ, Graves BJ. An ERK2 docking site in the Pointed domain distinguishes a subset of ETS transcription factors. Genes & development. 2002; 16:127–137. [PubMed: 11782450]

Stainier DY, Fouquet B, Chen JN, Warren KS, Weinstein BM, Meiler SE, Mohideen MA, Neuhauss SC, Solnica-Krezel L, Schier AF, et al. Mutations affecting the formation and function of the cardiovascular system in the zebrafish embryo. Development. 1996; 123:285–292. [PubMed: 9007248]

Stowe TR, Wilkinson CJ, Iqbal A, Stearns T. The centriolar satellite proteins Cep72 and Cep290 interact and are required for recruitment of BBS proteins to the cilium. Mol Biol Cell. 2012; 23:3322–3335. [PubMed: 22767577]

Su CY, Kemp HA, Moens CB. Cerebellar development in the absence of Gbx function in zebrafish. Dev Biol. 2014; 386:181–190. [PubMed: 24183937]

Summerton J, Weller D. Morpholino antisense oligomers: design, preparation, and properties. Antisense Nucleic Acid Drug Dev. 1997; 7:187–195. [PubMed: 9212909]

Summerton JE. Morpholino, siRNA, and S-DNA compared: impact of structure and mechanism of action on off-target effects and sequence specificity. Curr Top Med Chem. 2007; 7:651–660. [PubMed: 17430206]

Swift MR, Pham VN, Castranova D, Bell K, Poole RJ, Weinstein BM. SoxF factors and Notch regulate nr2f2 gene expression during venous differentiation in zebrafish. Dev Biol. 2014; 390:116–125. [PubMed: 24699544]

Tijssen MR, Cvejic A, Joshi A, Hannah RL, Ferreira R, Forrai A, Bellissimo DC, Oram SH, Smethurst PA, Wilson NK, et al. Genome-wide analysis of simultaneous GATA1/2, RUNX1, FLI1, and SCL binding in megakaryocytes identifies hematopoietic regulators. Dev Cell. 2011; 20:597–609. [PubMed: 21571218]

Traver D, Paw BH, Poss KD, Penberthy WT, Lin S, Zon LI. Transplantation and in vivo imaging of multilineage engraftment in zebrafish bloodless mutants. Nat Immunol. 2003; 4:1238–1246. [PubMed: 14608381]

Tse WK, Eisenhaber B, Ho SH, Ng Q, Eisenhaber F, Jiang YJ. Genome-wide loss-of-function analysis of deubiquitylating enzymes for zebrafish development. BMC Genomics. 2009; 10:637. [PubMed: 20040115]

Ulitsky I, Shkumatava A, Jan CH, Sive H, Bartel DP. Conserved function of lincRNAs in vertebrate embryonic development despite rapid sequence evolution. Cell. 2011; 147:1537–1550. [PubMed: 22196729]

van Impel A, Zhao Z, Hermkens DM, Roukens MG, Fischer JC, Peterson-Maduro J, Duckers H, Ober EA, Ingham PW, Schulte-Merker S. Divergence of zebrafish and mouse lymphatic cell fate specification pathways. Development. 2014; 141:1228–1238. [PubMed: 24523456]

Vettori A, Bergamin G, Moro E, Vazza G, Polo G, Tiso N, Argenton F, Mostacciuolo ML. Developmental defects and neuromuscular alterations due to mitofusin 2 gene (MFN2) silencing in zebrafish: a new model for Charcot-Marie-Tooth type 2A neuropathy. Neuromuscul Disord. 2011; 21:58–67. [PubMed: 20951042]

Wiens KM, Lee HL, Shimada H, Metcalf AE, Chao MY, Lien CL. Platelet-derived growth factor receptor beta is critical for zebrafish intersegmental vessel formation. PLoS One. 2010; 5:e11324. [PubMed: 20593033]

Yao S, Qian M, Deng S, Xie L, Yang H, Xiao C, Zhang T, Xu H, Zhao X, Wei YQ, et al. Kzp controls canonical Wnt8 signaling to modulate dorsoventral patterning during zebrafish gastrulation. The Journal of biological chemistry. 2010; 285:42086–42096. [PubMed: 20978132]

Yoo SK, Deng Q, Cavnar PJ, Wu YI, Hahn KM, Huttenlocher A. Differential regulation of protrusion and polarity by PI3K during neutrophil motility in live zebrafish. Dev Cell. 2010; 18:226–236. [PubMed: 20159593]

Yue R, Kang J, Zhao C, Hu W, Tang Y, Liu X, Pei G. Beta-arrestin1 regulates zebrafish hematopoiesis through binding to YY1 and relieving polycomb group repression. Cell. 2009; 139:535–546. [PubMed: 19879840]

Zhu C, Smith T, McNulty J, Rayla AL, Lakshmanan A, Siekmann AF, Buffardi M, Meng X, Shin J, Padmanabhan A, et al. Evaluation and application of modularly assembled zinc-finger nucleases in zebrafish. Development. 2011; 138:4555–4564. [PubMed: 21937602]

Zoeller JJ, McQuillan A, Whitelock J, Ho SY, Iozzo RV. A central function for perlecan in skeletal muscle and cardiovascular development. The Journal of cell biology. 2008; 181:381–394. [PubMed: 18426981]

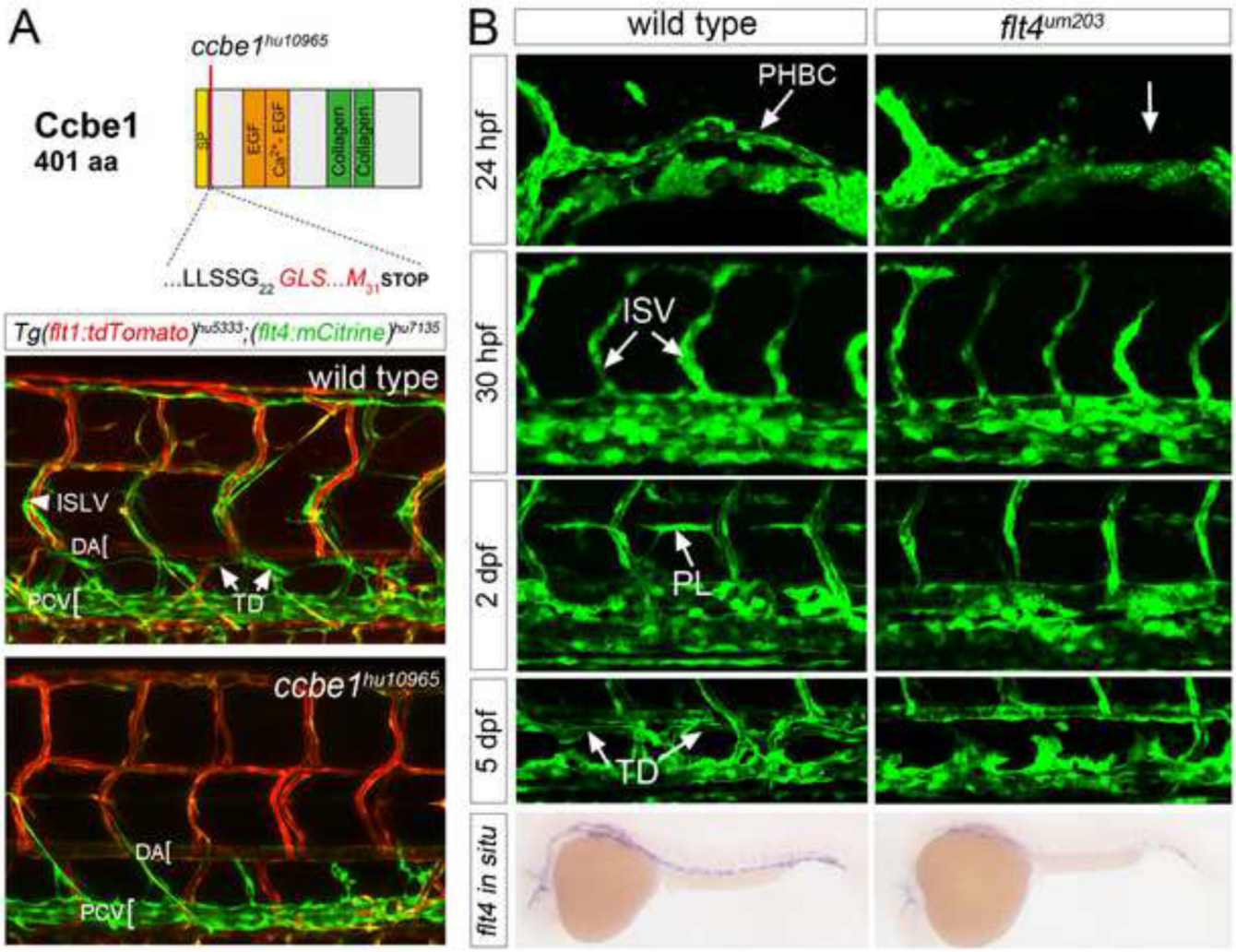

Figure 1.

TALEN-generated mutations in *ccbe1* and *flt4* cause lymphatic defects. (A) Schematic of Ccbe1 protein indicating position of the *ccbe1*^{hu10965} frame-shift. SP: Signal peptide, EGF: EGF-like domain, Ca^{2+}-EGF: Calcium-binding EGF-like domain, Collagen: Collagen-like domain. Images are confocal micrographs of wild type or *ccbe1*^{hu10965} mutant embryo bearing Tg(*flt4:mCitrine*)^{hu7135} (green) and *Tg(flt1:tdTomato)*^{hu5333} (red) transgenes. Homozygous *ccbe1*^{hu10965} mutants lack the thoracic duct (TD) and intersegmental lymphatic vessels (ISLV) at 5dpf; position of the dorsal aorta (DA) and posterior cardinal vein (PCV) are indicated. (B) Confocal micrographs of *Tg(fli1a:egfp)*^{y1} wild type and *flt4*^{um203} sibling embryos at 24 hpf, 30 hpf, 2 dpf, and 5 dpf. Positions of the primordial hindbrain channel (PHBC), intersegmental vessels (ISV), parachordal lymphangioblasts (PLs), and thoracic duct (TD) are indicated. All of these structures except ISVs are missing in *flt4*^{um203} mutants at indicated stages (right panels). Bottom panels show *flt4* transcript by whole mount *in situ* hybridization in wild type and *flt4*^{um203} mutant embryos at 28 hpf. (A,B) Lateral views, anterior to the left, dorsal is up.

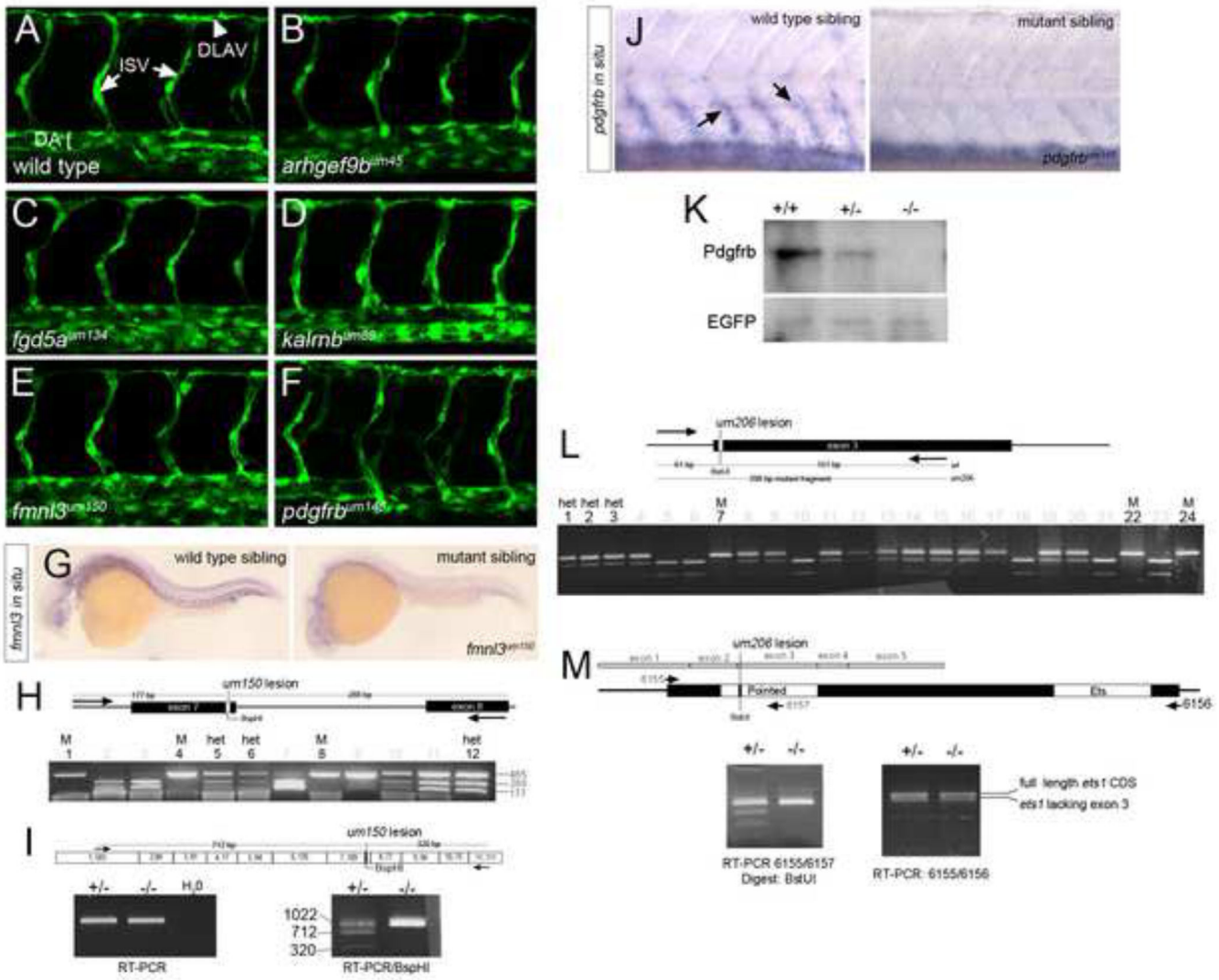

Figure 2.

Normal intersegmental vessel development in selected mutant embryos. (A-F) Confocal micrographs of *Tg(fli1a:egfp)*^{y1} or *Tg(kdrl:egfp)*^{s843}transgenic embryos at 32 hpf subjected to immunostaining with GFP antibody. (A) wild type sibling. Intersegmental vessels (ISV), dorsal longitudinal anastomotic vessel (DLAV) and dorsal aorta (DA) are indicated. (B-F) Embryos mutant for (B) *arhgef9b*^{um45}, (C) *fgd5a*^{um134}, (D) *kalrnb*^{um80}, (E) *fmnl3*^{um150}, or (F)*pdgfrb*^{um148}. (G) Whole mount *in situ* hybridization analysis of *fmnl3* wild type and *fmnl3*^{um150} mutant sibling at 26 hpf. (H) Schematic of *fmnl3* locus flanking *um150* allele and genotyping of individual embryo heads at 72 hpf from an incross of *fmnl3*^{um150} heterozygous carriers. Homozygous mutants and heterozygotes pooled for subsequent RT-PCR are indicated by an M and het, respectively. (I) Schematic of *fmnl3* transcript flanking *um150* and RT-PCR analysis of trunks from pooled M and het embryos shown in H. (J) Whole mount *in situ* hybridization analysis of *pdgfrb* in wild type and *pdgfrb*^{um148} mutants at 72 hours post fertilization. (K) Western blot analysis of Pdgfrb and Egfp in lysates from *Tg(fli1a:egfp)*^{y1};*pdgfrb*^{um148} of indicated genotype at 72 hpf. (L) Schematic of *ets1* exon 3

bearing the *um206* lesion and genotyping of individual embryo heads at 3 dpf from an incross of *ets1*^{um206} heterozygous carriers. (M) Schematic of *ets1* transcript and RT-PCR analysis of trunks from pooled M and het embryos shown in L. (A-G, J) Lateral views, dorsal is up, anterior to the left.

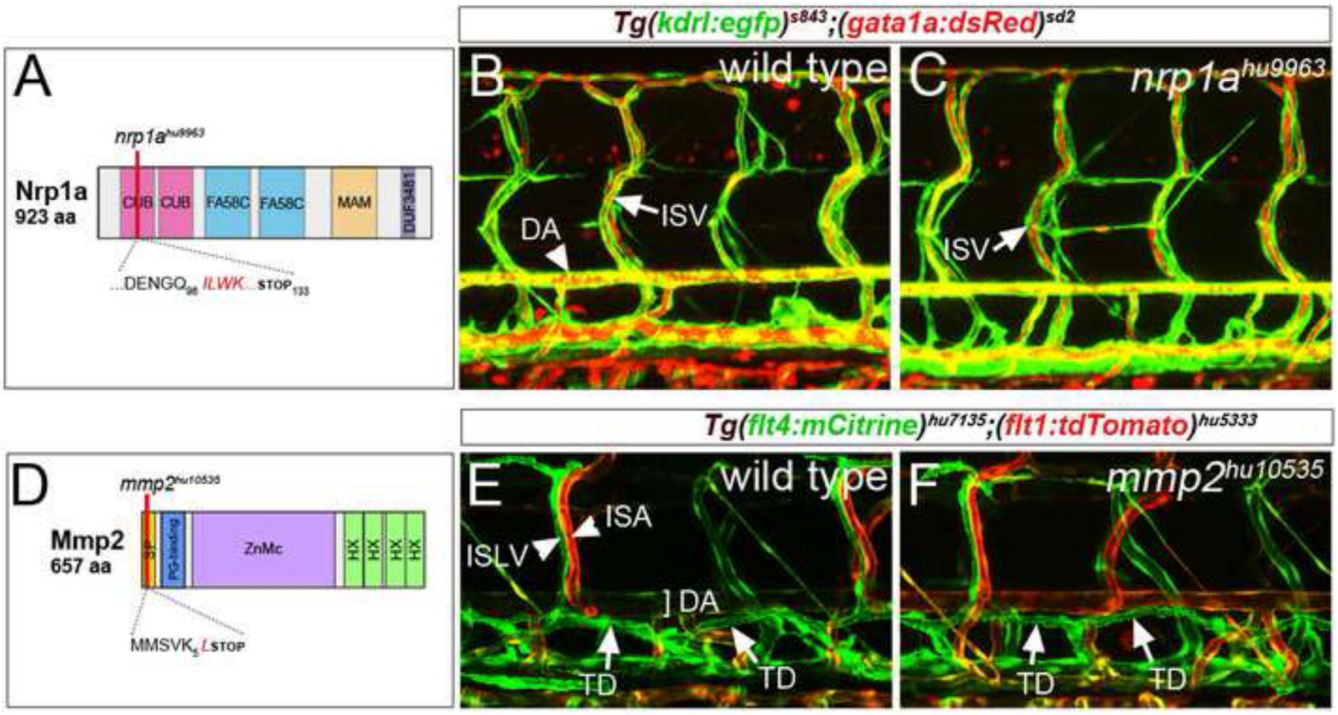

Figure 3.

Normal vascular and lymphatic development in *nrp1a* and *mmp2* mutant embryos. (A) Schematic of Nrp1a domain structure, indicating position of *nrp1a*^{hu9963}. CUB: CUB domain, FA58C: Coagulation factor 5/8 C-terminal domain, MAM: MAM domain, DUF3481: domain of unknown function. (B, C) Confocal micrograph of embryos bearing Tg(*kdrl:egfp*)^{s843} (green) and *Tg(gata1a:dsRed)*^{sd2} (red) transgenes at 5 dpf. (B) Wild-type. Dorsal aorta (DA) and intersegmental vessel (ISV) are indicated. (C) *nrp1a*^{hu9963} mutant. ISV carrying red blood cells is indicated. (D) Schematic of the Mmp2 and *mmp2*^{hu10535} allele. SP: Signal peptide, PG-binding: Peptidoglycan-binding domain, ZnMc: Zinc-dependent metalloprotease, HX: Hemopexin-like repeats. (E,F) Confocal micrographs of embryos bearing Tg(*flt4:mCitrine)*^{hu7135} (green) and *Tg(flt1:tdTomato)*^{hu5333} (red) transgenes. (E) Wild type. Intersegmental lymphatic vessel (ISLV), intersegmental artery (ISA), dorsal aorta (DA) and thoracic duct (TD) are indicated. (F) *mmp2*^{hu10535} mutant embryo.

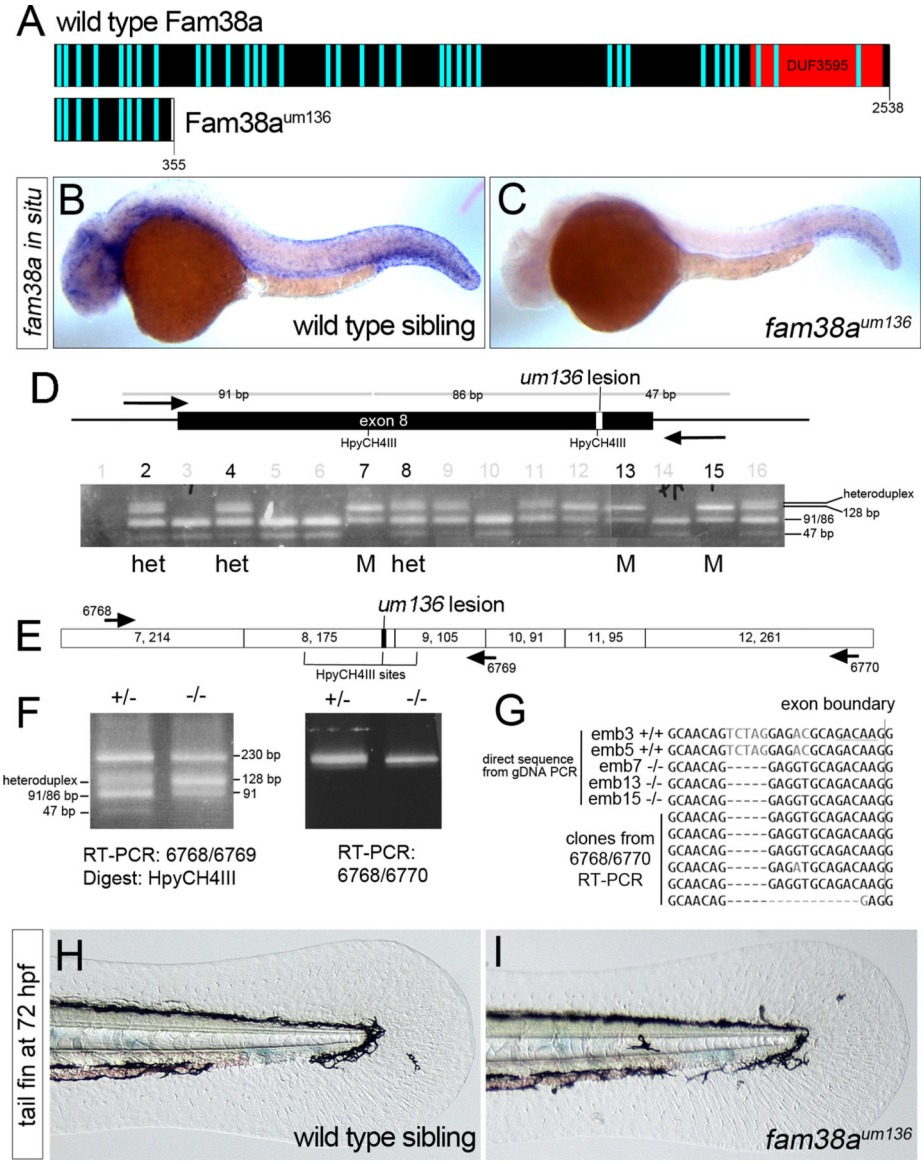

Figure 4.

Normal fin development in *fam38a* mutant embryos. (A) Schematic of Fam38a and truncated Fam38a^{um136}. Light blue bars - transmembrane domains. DUF- domain of unkown function. (B, C) Whole mount *in situ* hybridization of *fam38a* in (B) wild type and (C) *fam38a^{um136}* mutant at 28 hpf. (D) Schematic of *fam38a* exon 8 with *um136* lesion and genotyping of individual embryo heads at 72 hpf from an incross of *fam38a^{um136}* heterozygous carriers. Homozygous mutants and heterozygotes pooled for subsequent RT-PCR are indicated by an M and het, respectively. (E) Schematic of exons in *fam38a* transcript (numbers in each box indicate exon number, followed by exon size). (F) RT-PCR analysis of *fam38a* transcript in heterozygous and *fam38a^{um136}* mutant trunks pooled from the het and M embryos in (D). (G) Top five sequences are directly from PCR products from genomic DNA of numbered individuals in (D). HpyCH4III site is underlined and the 5bp *um136* deletion is evident. Bottom 6 sequences are cloned fragments from RT-PCR of

pooled *fam38a*^{um136} mutant embryos (embryos 7, 13, and 15). (H, I) Transmitted light images of the tail fin fold in live (H) wild type and (I) *fam38a*^{um136} mutant embryos at 72 hpf.

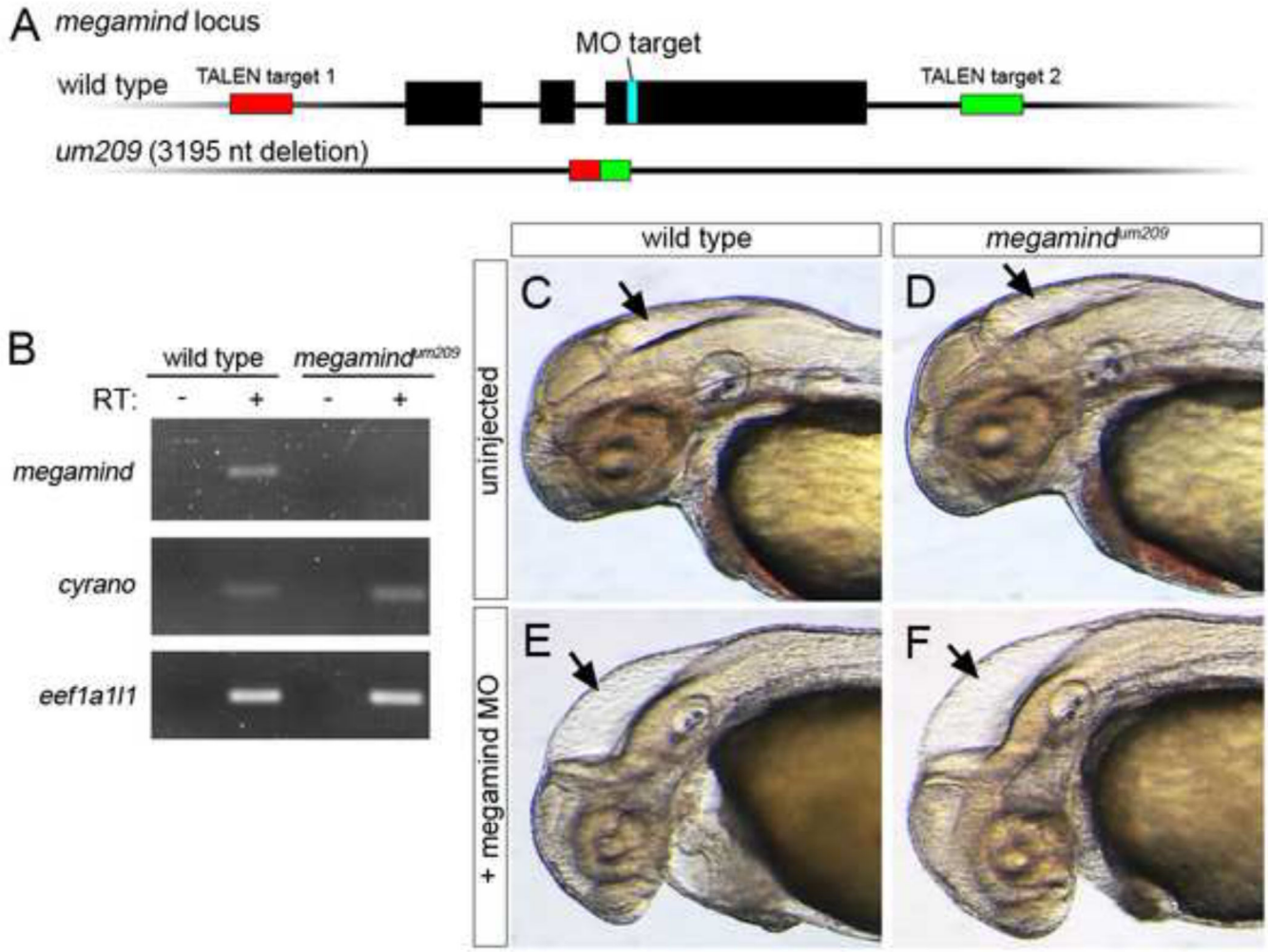

Figure 5.

Normal hindbrain development in *megamind* mutant embryos. (A) Schematic of the *megamind* locus in wild type and *megamind*^{um209} mutants. The red and green boxes indicate relative position of the TALEN target sequences and the MO target sequence is shown. (B) RT-PCR for the *megamind* and *cyrano* lincRNAs, as well as *eef1al1* in wild type and *megamind*^{um209} mutant embryos. RT – refers to RNA template without (−) or with (+) reverse transcription. (C-F) Transmitted light images of the head region in embryos at 48 hpf. The hindbrain ventricle is indicated with an arrow in each panel. Lateral views, anterior to the left, dorsal is up. (C) Wild type, uninjected. (D) *megamind*^{um209} mutant, (E) Wild type injected with 20 ng *megamind* conserved site MO. (F) *megamind*^{um209} mutant injected with *megamind* conserved site MO.

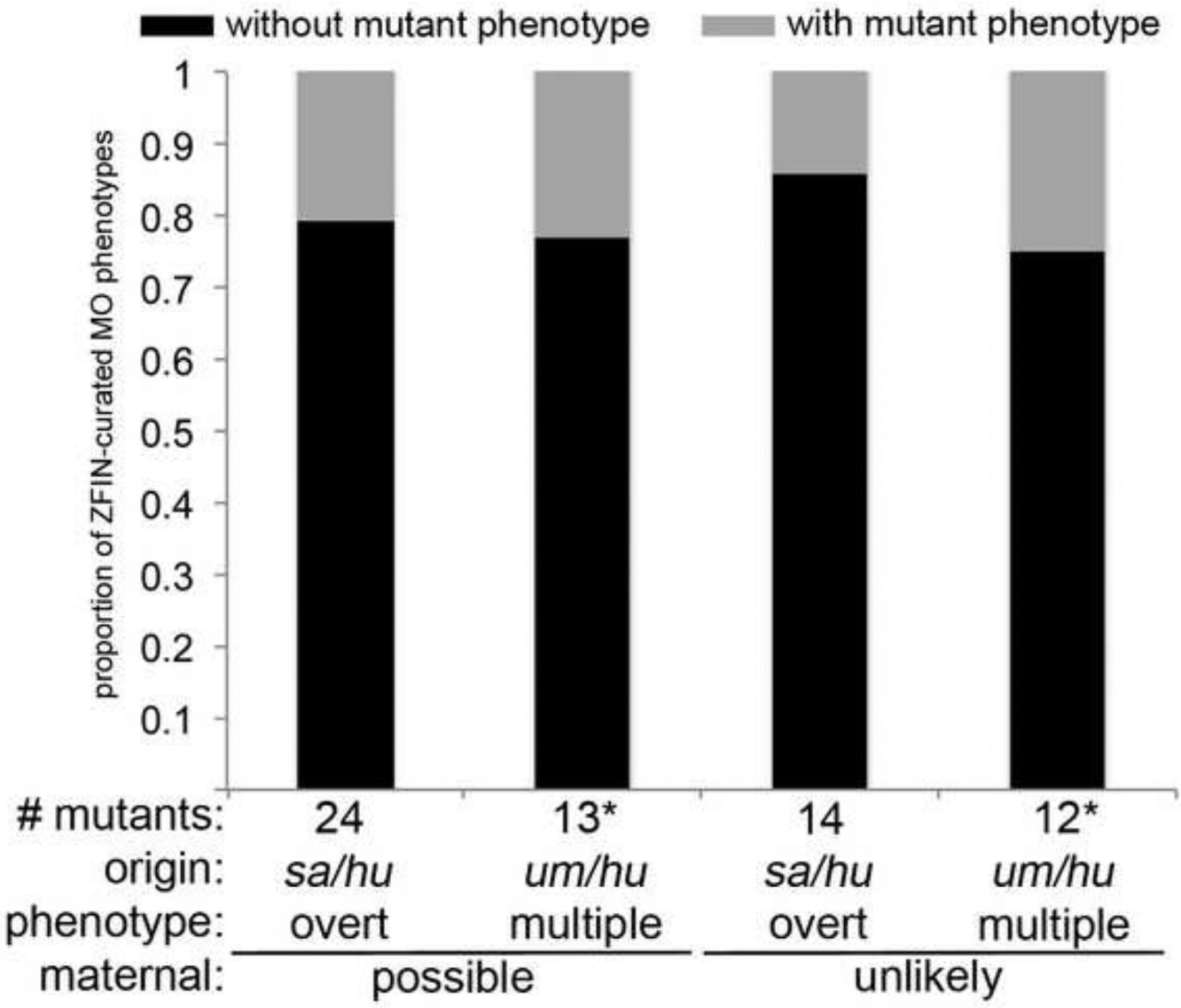

Figure 6.

Results of integrative analysis of Sanger Center and ZFIN-curated mutant and morphant datasets. Graph shows proportion of all genes with associated morphant phenotypes that display or do not display a corresponding mutant phenotype. * - *flt4* is included in both categories (with and without mutant phenotype) as lymphatic defects match the mutant, while ISV defects do not. Allele designations: *hu* – Hubrecht Institute, *sa* – Sanger Center, *um* – UMass Medical School

Table 1

Inconsistencies between morphant and mutant phenotypes.

Morphants with specific phenotypes

	Morphant			Mutant	
Gene	**phenotype**	**Resc.**	**Reference**	**Zygotic phenotype**	**Source**
flt4	loss of lymphatics; stalled ISVs	ND	(Covassin et al., 2006)	loss of lymphatics	um
ccbe1	loss of lymphatics	ND	(Hogan et al., 2009a)	loss of lymphatics	hu
gata2a	lack of trunk circulation at 48 hpf	ND	(Fiedler et al., 2011)	lack of trunk circulation	um
amot	stalled ISVs	Yes	(Aase et al., 2007)	Normal	um
elmo1	stalled ISVs	Yes	(Epting et al., 2010)	Normal	um
ets1	stalled ISVs, no circulation at 48 hpf	ND	(Pham et al., 2007)	Normal	um
fmnl3	stalled ISVs	Yes	(Hetheridge et al., 2012)	Normal	um
mmp2	loss of lymphatics	ND	(Detry et al., 2012)	Normal	hu
nrp1a	ISV stalling and mispatterning	ND	(Martyn and Schulte-Merker, 2004)	Normal[1]	hu
pdgfrb	ISV stalling	Yes	(Wiens et al., 2010)	Normal	hu

Morphants with overt phenotypes

	Morphant			Mutant	
Gene	**phenotype**	**Resc.**	**Reference**	**Zygotic phenotype**	**Source**
bmp7a	dorsalized	ND	(Lele et al., 2001)	dorsalized	sa
ttna	decreased heartbeat; edema	ND	(Seeley et al., 2007)	loss of heartbeat	sa
dag1	dystrophic	ND	(Parsons et al., 2002a)	dystrophic[1]	sa
lamc1	decreased length	ND	(Parsons et al., 2002b)	decreased length[1]	sa
tll1	dorsalized; loss of tail fin	ND	(Lele et al., 2001)	dorsalized; loss of tail fin[1]	sa
fam38a	gastrulation defective; fin blistering	ND	(Eisenhoffer et al., 2012)	Normal	um
linc:birc6	hindbrain ventricle inflation	Yes	(Ulitsky et al., 2011)	Normal	um
appl1	necrosis, short yolk extension	Yes	(Schenck et al., 2008)	Normal[1]	sa
arrb1	severe delay and necrosis	Yes	(Yue et al., 2009)	Normal	sa
bmper	severe trunk malformation	ND	(Moser et al., 2007)	Normal	sa
ccdc78	curved and shortened trunk	ND	(Majczenko et al., 2012)	Normal	sa
cep290	cystic and slight curvature	ND	(Sayer et al., 2006)	Normal	sa
col2a1a	curved trunk	ND	(Mangos et al., 2010)	Normal	sa
hsp90ab1	shortened axis	ND	(Pei et al., 2007)	Normal[1]	sa
glcci1	curved trunk	Yes	(Nishibori et al., 2011)	Normal	sa
hspg2	curved and shortened trunk	Yes	(Zoeller et al., 2008)	Normal	sa
htra1a	dorsalized	ND	(Kim et al., 2012a)	Normal	sa
lratb	shortened and necrotic	Yes	(Isken et al., 2007)	Normal[1]	sa
itga2b	curved trunk	ND	(San Antonio et al., 2009)	Normal	sa
nrp1a	curved trunk	ND	(Hillman et al., 2011)	Normal[1]	sa
pcm1	curved, cystic	Yes	(Stowe et al., 2012)	Normal[1]	sa
mfn2	hindbrain ventricle inflation; curved trunk	Yes	(Vettori et al., 2011)	Normal	sa
ptenb	kinked trunk/tail	ND	(Croushore et al., 2005)	Normal	sa

Morphants with overt phenotypes

	Morphant			Mutant	
Gene	**phenotype**	**Resc.**	**Reference**	**Zygotic phenotype**	**Source**
ptger4a	shortened axis	Yes	(Cha et al., 2006)	Normal	sa
usp33	CNS necrosis, curved trunk	ND	(Tse et al., 2009)	Normal[1]	sa
zbtb4	dorsalized	Yes	(Yao et al., 2010)	Normal[1]	sa

ND – not determined; 1 – possible maternal contribution; um – UMass Medical School; hu – Hubrecht Institute; Sa – Sanger Zebrafish Mutation Project